Journal of Cellular Biochemistry 48:203–214 (1992)

Rate Transition and Regulatory Coupling in Endocytosis of Interferon-α and Tumor Necrosis Factor-α in Human Epithelial Tumor Cells

Željko Bajzer and Stanimir Vuk-Pavlović

Division of Developmental Oncology Research (S.V.-P.) and Department of Biochemistry and Molecular Biology (Ž.B., S.V.-P.), Mayo Clinic and Foundation, Rochester, Minnesota 55905

Abstract The time-dependent concentrations of interferon-α and tumor necrosis factor-α associated with the membrane and internalized by cells contain information on the kinetics of endocytosis and their cellular processing. This information can be reduced quantitatively by application of the respective compartmental models. In our studies of human epithelial tumor cells interacting with human interferon-α and human tumor necrosis factor-α, we accounted only for actual endocytosis and elimination of the tracer from cells by a novel method sensitive to changes in the rate of endocytosis, to the delay in tracer elimination, and to the nonlinear regulatory coupling between endocytosis and the internalized ligand. Data reduced by this method resulted in best-fit parameter values statistically superior to values obtained by previous methods (Bajzer et al., 1989). The results indicate a change with time in the rate of endocytosis of tumor necrosis factor-α and the inhibition of endocytosis by the endocytosed ligand-receptor complex. We conclude that sorting and processing of interferon-α and tumor necrosis factor-α are restricted by the type of both the receptor and the cell.

Key words: endocytosis, regulatory coupling, kinetic models, nested models

To convey information or deliver nutrients to cells, specific proteins bind to receptors at the cell surface. Binding results in formation of ligand-receptor complexes which are transferred to cellular interior by endocytosis. Endocytosis is believed to regulate communication and nutrient transfer between the cell and the environment [cf. reviews by Klausner et al., 1985; Goldstein et al., 1985; Owensby et al., 1989].

The regulatory function of endocytosis is exemplified by depletion ("down-regulation") of receptors after binding of growth factors and protein hormones; this process limits cellular response to subsequent exposure to the ligand. Regulation of numbers of receptors for insulin and epidermal growth factor by their respective ligands provides the well-documented paradigms for this mechanism (cf. Gordon et al., 1989; Lund et al., 1990). Levels of membrane receptors and endocytosis of ligand-receptor complexes can also be regulated via heterologous receptors. For example, specific binding of epidermal growth factor, insulin, insulin-like growth factor I, and platelet-derived growth factor regulates the levels of membrane receptors for transferrin and rates of transferrin-mediated iron loading into cells (Davis and Czech, 1986; Davis et al., 1987).

Inherent to regulation of endocytosis are changes in the rates of constitutive elementary processes. For instance, receptor levels in the cell membrane are increased when the rate of endocytosis is reduced, when the rate of their insertion into the membrane is increased, or both. Therefore, an understanding of the kinetics of these processes is required for unraveling endocytotic regulation and for its rational manipulation.

There have been numerous attempts to manipulate the membrane receptors for treatment of malignant cells by biological response modifiers (BRMs) or to deliver cytotoxic agents into the cytoplasm by receptor-mediated endocytosis (for review, see FitzGerald and Pastan, 1989). We have been interested in regulation of endocytosis of BRMs by human tumor cells under conditions of potential interest for therapy. We have particularly studied human recombinant interferon-α_2a (IFN) and human recombinant tumor

Received April 4, 1991; accepted September 26, 1991.

Željko Bajzer is on leave of absence from the Rugjer Bošković Institute, Zagreb, Croatia, Yugoslavia.

necrosis factor-α (TNF) interacting with tumor cells in the course of hours (Myers et al., 1987; Bajzer et al., 1989; Vuk-Pavlović and Kovach, 1989; Dunne et al., 1990). Although effects of such long exposures of cells to BRMs might influence regulation of endocytosis (e.g., by poisoning the endocytotic apparatus by internalized ligand or by ligand-induced receptor synthesis), they have not been completely understood. We believe that the understanding of the kinetics of these regulatory phenomena might contribute to optimization of interactions of BRMs and immunotoxins with tumor cells.

The interest in the kinetics of endocytosis prompted the development of specific experimental techniques and methods for quantitative data reduction. In a typical experiment, the time-dependent concentrations of the ligand (usually radioactively labeled) bound to the surface receptors and the concentrations of endocytosed ligand are measured. This scheme has been widely used since the introduction of a simple acid wash method for removal of radioactive ligands from the cellular membrane (Haigler et al., 1980).

Information inherent in the time-dependent concentrations of membrane associated radioactivity and internalized radioactivity can be deduced by fitting to data the functions of compartmental models of receptor metabolism (Wiley and Cunningham, 1981; Ciechanover et al., 1983; Gex-Fabry and DeLisi, 1984; Lauffenburger et al., 1987; Myers et al., 1987; Beck, 1988; Bajzer et al., 1989; Waters et al., 1990). These models are based on experimentally supported kinetic steps in receptor metabolism and have been implemented for evaluation of parameters characteristic of ligand-receptor kinetics after introduction of the ligand to cells. However, the analysis of interdependence of variables and best-fit parameter values indicated that some parameters were insensitive (Bajzer et al., 1989; Waters et al., 1990). Therefore, it would be advantageous to define a model or models with a smaller number of more sensitive parameters characterizing processes particularly interesting and important to students of endocytosis.

Opresko and Wiley (1987) proposed a method for evaluation of the endocytotic rate constant k_e. By this method, k_e is evaluated from the slope of the line representing the total internalized ligand as a function of integrated surface-associated ligand. This simple and practical approach is not adequate, however, when the relationship between the total internalized ligand and integrated surface-associated ligand is not linear (e.g., when cells eliminate the internalized ligand) (Waters et al., 1990). To account for the sources of nonlinearity, we extended the model by Opresko and Wiley (1987) to include elimination of internalized ligand, the change in endocytotic rate and the nonlinear regulatory coupling in endocytosis.

The scope of this work was to analyze the paradigms for interactions of human epithelial carcinoma cells with recombinant human interferon-α_2a and recombinant human tumor necrosis factor-α. Particularly, we evaluated the endocytotic rates and the regulatory coupling between internalized ligand-receptor complexes and surface receptors and compared the results with those obtained previously by more standard compartmental modeling (Myers et al., 1987; Bajzer et al., 1989). For this analysis we developed and applied a set of nested models of receptor metabolism characterized by the minimum number of statistically meaningful parameters and formally independent of ligand binding to receptors. These parameters were obtained by fitting the model functions to time-dependent membrane-associated radioactivity and internalized radioactivity only.

EXPERIMENTAL PROCEDURES

The protocol for evaluation of interactions of human lung alveolar carcinoma A549 cells and human melanoma A101D cells with IFN and TNF was described by Myers et al. (1987), Bajzer et al. (1989), and Dunne et al. (1990), respectively. Briefly, recombinant human interferon-α_2a (Hoffman-LaRoche, Nutley, NJ) was labeled with ^{125}I to the specific radioactivity of 1.6×10^{16} Bq/mol and recombinant human tumor necrosis factor-α (Genentech, San Francisco, CA) to the specific radioactivity of 1.1×10^{16} Bq/mol. Experiments were initiated by the introduction of ^{125}I-IFN (9.4×10^{-11} M) or ^{125}I-TNF (1.5×10^{-10} M) to confluent cells at 37°C. Under these conditions, less than 5% of the ligand was metabolized by cells during the experiment. At selected times the cells were placed on ice, washed free of unbound radioactivity and stripped from dissociable radioactivity by the cold acid wash (200 mM acetic acid, 0.5 M sodium chloride, pH 2.5; Haigler et al., 1980). Radioactivity in the acid wash was counted and taken to represent radioactivity associated with the cellular surface. Radioactivity remaining with cells after the acid wash was taken to represent internalized radioactivity. Data in Figures

3a, 4a, and 5a are corrected for the nonspecific binding and internalization. The nonspecific effects were determined as surface-associated radioactivity and internalized radioactivity in the presence of 1.1×10^{-7} M native ligand; these effects did not exceed 10% of the corresponding value measured in the absence of native ligand. Each experiment was repeated three times with reproducible time dependence of surface-associated and internalized radioactivity.

The results are presented in Figure 3a, 4a, and 5a as surface-associated and internalized radioactivity as a function of time. The solid traces in these figures connect the best-fit points of internalized radioactivity obtained by fitting Eq. (9) to original data (rather than to transformed data in Figs. 3b, 4b, and 5b). For comparison with the results of previous studies, data in Figure 3a and 4a were taken from Figure 2 in Myers et al. (1987) and Figure 3 in Bajzer et al. (1989).

RESULTS

The Model of Endocytosis and Estimation of Parameters

Assumptions of the model. We propose a generalized model of endocytosis which includes a set of nested models. The models are nested in that each encompasses its parent model and one additional kinetic process and are based on the following assumptions:

1. Endocytosis is a linear process with respect to concentration of ligand-receptor complex at the cell surface (Wiley and Cunningham, 1981). It can be characterized by two rate constants: k_{e1} (for times less than T_c) and k_{e2} (for times larger than T_c).

2. Concentration of internalized ligand and endocytosis are coupled. This means that: i) the concentration of internalized ligand depends on the rate of endocytosis, and ii) the rate of endocytosis is affected by the concentration of internalized ligand. The coupling is characterized by the constant *c*, which, if smaller than zero, describes the negative feedback (in a broad sense) and, if larger than zero, the positive feedback. Note, however, that the constant c is a phenomenological parameter encompassing *all* particular molecular mechanisms in regulatory coupling.

3. Elimination of internalized radioactivity is a linear function of internalized radioactivity and is characterized by the rate constant k_h (Wiley and Cunningham, 1981) and time delay T_h.

The basic model includes a single endocytotic rate constant. The next level of complexity introduces one more rate process (e.g., elimination of radioactivity from cells) or the second endocytotic rate constant. In the selection of an appropriate minimal model for description of a particular data set, we apply the parsimony (stinginess) principle defined as selection of the simplest model that reveals the least amount of information not already known or expected. This principle, standard in modeling, guards against overinterpretation of data.

Schematic and mathematical formulation of the model. We constructed a two-compartment model to include the above assumptions. The two compartments are the compartment of ligand-receptor complex at the cell surface (measured as surface radioactivity, $[LR]_s$) and the compartment of internalized ligand (comprising the ligand-receptor complex, the dissociated ligand, and the degraded ligand; measured as internalized radioactivity, $[LR]_i$). The model is shown schematically in Figure 1.

The mathematical formulation of the model is based on the fundamental equation

$$\frac{d[LR]_i}{dt} = R_{in} - R_{el}, \qquad (1)$$

which specifies the change of internalized radioactivity as the difference of ligand-receptor internalization rate R_{in} and internalized radioactivity elimination rate R_{el}. Assumption 1, expressed in the language of compartmental modeling (Jacquez, 1985), leads to

$$R_{in} = k_e(t)[LR]_s(t), \qquad (2)$$

where (cf. Eq. 5 in Gex-Fabry and DeLisi, 1984)

$$k_e(t) = k_{e1} + (k_{e2} - k_{e1})d(t, T_c, N), \qquad (3)$$

$$d(t, T, N) = 1 - e^{-(t/T)^N}, N = 3, 5, 7, \ldots \qquad (4)$$

Here the function $d(t, T_c, N)$ permits the rate constant k_{e1} to go over smoothly to the rate constant k_{e2}. The larger the exponent N, the more sudden the transition (Fig. 1).

To implement Assumption 2, we modify R_{in} given by Eq. (2) to depend on internalized radioactivity too. This is accomplished by the introduction of factor $\varphi > 0$ dependent on $[LR]_i$ so that R_{in} can be generally expressed as:

$$R_{in} = k_e(t)[LR]_s(t)\varphi([LR]_i). \qquad (5)$$

If coupling between the internalization rate R_{in} and internalized radioactivity $[LR]_i$ is negligible,

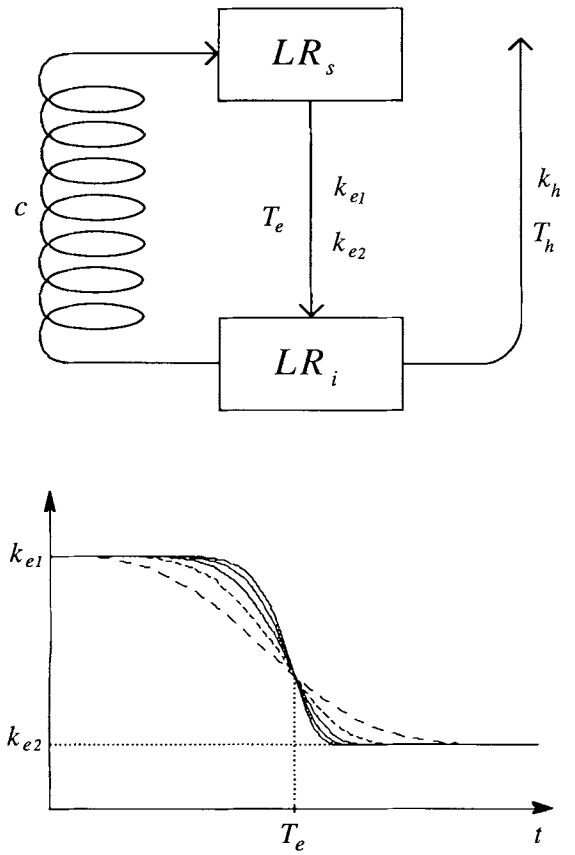

Fig. 1. Compartmental model of endocytosis. **Upper panel:** Ligand-receptor complexes at the cell surface (LR_s) are endocytosed into the compartment of internalized radioactivity (LR_i) by the process characterized by rate constants k_{e1} and k_{e2}. The transition from k_{e1} regimen to k_{e2} regimen occurs at the mean transition time T_e. Radioactivity is eliminated from the compartment LR_i by the process characterized by k_h with the mean delay time T_h. The constant c characterizes the coupling (symbolized by the spiral) of LR_i and the rate of endocytosis. **Lower panel:** Transition from k_{e1} to k_{e2} in time for different values of N in Eq. 3. The shallowest (dashed) curve was obtained with N = 3. Further increase in N (5, 7, 9, and 11) resulted in sequentially steeper curves.

$\phi([LR]_i)$ equals one. Also, it is reasonable to assume that $\varphi(0) = 1$. The selection of function $\varphi(x)$ can then be guided by its Taylor expansion: $\varphi(x) = 1 + c_1x + c_2x^2 + \ldots$. However, in general, a better approximation of $\varphi(x)$ can be achieved by use of Padé approximants (Bender and Orszag, 1978; Press et al. 1986). Specifically, we can choose $\varphi(x)$ to be represented by its [0,1] Padé approximant: $1/(1 - cx)$. Such selection complies with Assumption 2 that coupling be described by one constant and is analogous to the "magnification factor" known from the theory of feedback mechanisms (Riggs, 1966). In addition, a nonlinear dependence of factor φ on the coupling constant c prevents redundancy in adjustable parameters.

In the spirit of compartmental modeling (Jacquez, 1986), Assumption 3 can be formulated as

$$R_{el} = k(t)[LR]_i(t), \quad k(t) = k_h d(t, T_h, N). \quad (6)$$

Combining Eqs. (1), (5), and (6) and selecting the proposed Padé approximant for φ, we can explicitly write the equation for the change of internalized radioactivity as:

$$\frac{d[LR]_i(t)}{dt} = \frac{k_e(t)[LR]_s(t)}{1 - c[LR]_s(t)} - k(t)[LR]_i(t). \quad (7)$$

This equation represents a substantial generalization of the model proposed by Opresko and Wiley (1987). When $k_e(t) = k_{e1}$, $c = 0$, $k(t) = 0$, Eq. (7) yields their original model:

$$\frac{d[LR]_i(t)}{dt} = k_{e1}[LR]_s(t). \quad (8)$$

From the integrated form of Eq. (8) it follows that the model predicts a linear dependence of $[LR]_s$ on the integral of $[LR]_s$. Such dependence has been documented by Opresko and Wiley (1987) for incubation times shorter than the onset of elimination (T_h). Our model defined by Eq. (7) predicts a *nonlinear* dependence of $[LR]_i$ on the integral of $[LR]_s$. This prediction is supported by measurements in cells incubated with ligands for times longer than T_h (see below).

Estimation of model parameters. Let $[LR]_s$ and $[LR]_s$ be measured at times $t = t_1 \ldots t_n$. To estimate the model parameters, first we integrate Eq. (7) from time t_1 to time t_j:

$$[LR]_i(t_j) = k_{e1}F(t_j) + k_{e2}G(t)_j - k_hH(t_j) + [LR]_i(t_1), \quad j = 1, \ldots, n \quad (9)$$

where

$$F(t_j) = \int_{t_1}^{t_j} \frac{1 - d(t, T_e, N)}{1 - c[LR]_i(t)} [LR]_s(t)\, dt, \quad (10)$$

$$G(t_j) = \int_{t_1}^{t_j} \frac{d(t, T_e, N)[LR]_s(t)}{1 - c[LR]_i(t)} dt, \quad (11)$$

$$H(t_j) = \int_{t_1}^{t_j} d(t, T_h, N)[LR]_i(t)\, dt. \quad (12)$$

The integrals F, G, and H can be evaluated by use of measured data and trapezoidal integration rule. In this way, the left hand side of Eq. (9) depends only on model parameters: k_{e1}, k_{e2},

T_e, c, k_h, and T_h. These can be now determined by minimization of the χ^2 function:

$$\chi^2 = \sum_{j=1}^{n} \{[LR]_i^{exp}(t_j) - [LR]_i(t_j)\}^2/\sigma_j^2, \quad (13)$$

where $[LR]_i^{exp}(t_j)$ is the measured internalized radioactivity at time t_j with the standard error σ_j; $[LR]_i(t_j)$ is given by Eq. (9) with $[LR]_i(t_1)$ replaced by $[LR]_i^{exp}(t_1)$.

Estimation of the only parameter in the simple model of Opresko and Wiley (1987) (cf. Eq. 8) is straightforward; minimization of the corresponding χ^2 function can be performed analytically to yield

$$k_{e1} = \frac{\sum_{j=2}^{n} [LR]_i^{exp}(t_j) I(t_j)/\sigma_j^2}{\sum_{j=2}^{n} [I(t_j)/\sigma_j]^2}, \quad (14)$$

$$I(t_j) = \int_{t_1}^{t_i} [LR]_s(t)\, dt. \quad (15)$$

However, estimation of parameters in our model requires numerical minimization.

Equation (7) describes a set of the total of 64 nested models characterized by all possible combinations of free parameters and parameters fixed to zero. From this comprehensive set we selected the biologically meaningful models only (Fig. 2). For models including both k_{e1} and k_{e2} and/or k_h, we eliminated parameter combinations devoid of corresponding delays T_e and T_h, respectively. The only exception was Model 1 included for comparison with previous results (Myers et al., 1987; Dunne et al., 1990). The nesting scheme for these models is presented in Figure 2.

Computational and statistical methods. Difficulties inherent to numerical minimization of a nonlinear function of several variables rapidly increase with the number of variables. Therefore, it is advantageous when the specific form of the function allows the number of variables to be reduced by specific procedures. In case of the χ^2 function (13), for the given values of c, T_e, and T_h, one can find k_{e1}, k_{e2}, and k_h, which minimize this function by use of matrix algebra (the linear least square problem). Thus, the nonlinear minimization is performed only with respect to variables c, T_e, and T_h. This approach is somewhat complicated by the obvious requirement for the rate constants k_{e1}, k_{e2}, and k_h to be nonnegative, so that the linear least square solution with nonnegativity constraints (Lawson and Hanson, 1974) must be found. However, even with this numerical complication such an approach is more efficient than the nonlinear minimization with respect to all six variables. Specifically, we used the subroutine by Haskell and Hanson (Morris, 1981) for the linear least square problem with nonnegativity constraints and Nelder-Mead simplex algorithm for nonlinear minimization (implementation of Press et al., 1986).

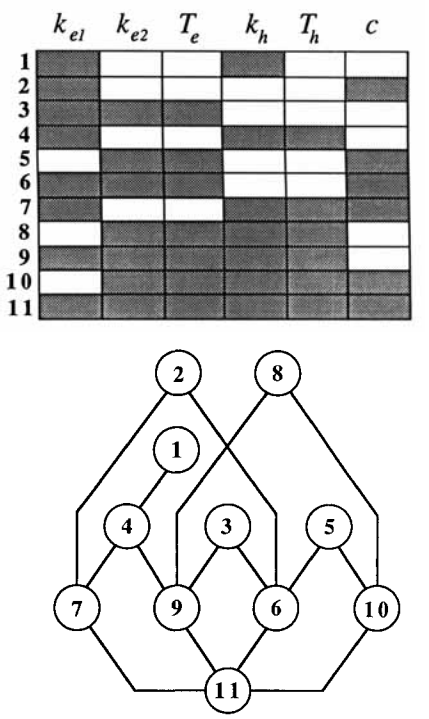

Fig. 2. Nested models of endocytosis. **Upper panel:** Schematic representation of parameter combinations in nested Models 1 through 11. Shaded areas represent free parameters. **Lower panel:** Nesting scheme for Models 1 through 11.

Parameters k_{e1}, k_{e2}, T_e, k_h, T_h, and c were estimated for different fixed values of "smoothness-of-transition" parameter N (= 3, 5, 7, 9, 11; cf. Eq. 4). From these results we selected the optimum value of N characterized by the smallest χ^2 and by the absence of change in best-fit parameter values upon further increase in N. For fits in this paper, N = 7 was optimal.

Together with determination of the best-fit parameter values which characterize endocytosis, we also estimated the uncertainties in parameters. Because our approach involves integration over measured quantities (with errors of

measurement), any classical way of determining uncertainties in estimated parameters by use of variance-covariance matrix may not be reliable. Therefore, we used a variant of the Monte Carlo method (cf. Press et al., 1986). Assuming that errors in measurement of surface-associated and internalized radioactivity follow a Gaussian distribution, we simulated a number of data curves (for internalized and surface-associated radioactivity) and analyzed them analogously as the original data curves. The procedure led to an approximate distribution for each parameter; these distributions were then used to estimate uncertainties in obtained parameter values. Specifically, if for some parameter p the best fit value for original data was p_o and the best fit values for simulated data were $p_1, \ldots, p_m$, the uncertainty associated with parameter p was estimated as

$$\sigma_p = \sqrt{\sum_{i=1}^{m} (p_o - p_i)^2/m} \qquad (16)$$

and expressed as the coefficient of variability $100\sigma_p/p_o$. Clearly, the greater the number of simulations m, the better the uncertainty estimate. In this report we used m = 100, but in most cases m = 50 provided sufficiently robust uncertainty estimates.

With the best-fit parameters and χ^2 values for the series of nested models evaluated, the most adequate model must be selected. The selection proceeds in the following steps: First, the fits characterized by the high outlying χ^2 values are eliminated. Then, the fits with the lowest χ^2 values are selected for each subset of models with the same number of parameters. The final selection is guided by the F-test for nested models (Bevington, 1969; Cook and Weisberg, 1990), by the a priori knowledge and by the principle of parsimony. The F-test establishes the probability level for the difference between the fits of two different models to the same data. It is based on the statistic

$$f = \frac{\mu_2[\chi^2(m_1) - \chi^2(m_2)]}{\mu_1\chi^2(m_2)},$$

$$\mu_2 = n - m_2, \quad \mu_1 = m_2 - m_1, \qquad (17)$$

which follows approximately the F-distribution with μ_1 and μ_2 degrees of freedom: $F(\mu_1, \mu_2; \chi)$. Here the values of $\chi^2(m_1)$ and $\chi^2(m_2)$ correspond to the minimal χ^2 values obtained for the nested models defined by m_1 and m_2 free parameters, respectively ($m_2 > m_1$). The probability of rejecting the true hypothesis "two fits are equivalent" is calculated as: $P = 1 - F(\mu_1, \mu_2; f)$, where f is given by Eq. (17) (for numerical evaluation of F-distribution, see e.g. Press et al., 1986). The smaller the value of P, the less likely the statistical equivalence of the fits.

Endocytosis of IFN and TNF by Human Epithelial Carcinoma Cells

Interactions of A549 cells with IFN: Single endocytotic rate with elimination of radioactivity. The plot in Figure 3b represents internalized radioactivity as a function of integrated surface radioactivity. This plot deviates from linearity, but the role of particular

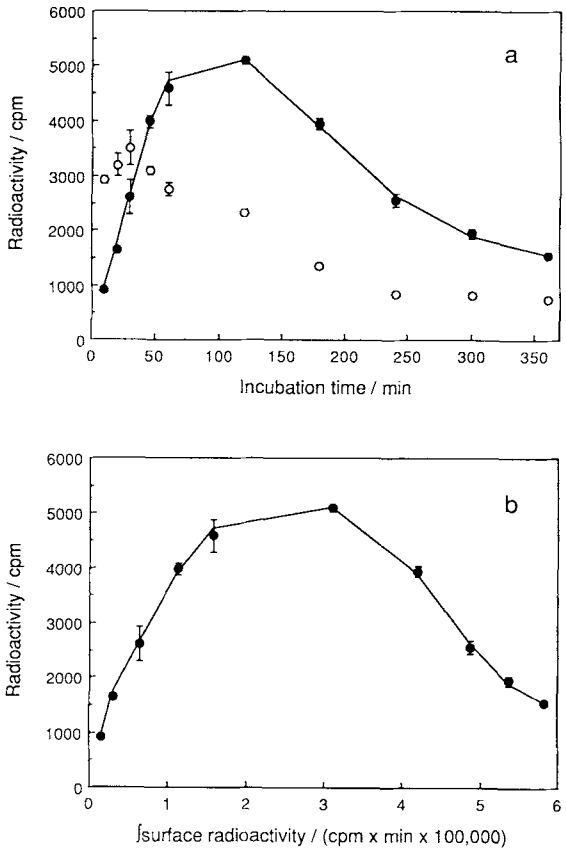

Fig. 3. Binding and internalization of ^{125}I-interferon-α_2a. **Panel a:** Surface-associated (circle lines) and internalized (full circles) radioactivity were measured as a function of time at 37°C. The solid line represents the best fit of Eq. (9) to data. The broken line results from the application of trapezoidal integration rule. **Panel b:** Data from panel a transformed to show internalized radioactivity as a nonlinear function of integrated surface-associated radioactivity (Eq. 15).

elementary processes (characterized by k_{e1}, k_{e2}, k_h, and c) in this nonlinear behavior is not readily apparent. To probe for relative contribution of these processes, we evaluated the series of nested models increasing in complexity (Fig. 2) by fitting model functions to data. The best-fit parameter values are displayed in Table I.

An inspection of Table I reveals that fits of different models resulted in different χ^2 values. These values are grouped in two sets. The set characterized by $\chi^2 \geq 23$ (Models 1, 2, 3, 5, and 6) was readily rejected because the other set consisted of significantly lower χ^2 values (1.6 to 6.3). Models 4 (three parameters), 7 and 8 (four parameters), 9 and 10 (five parameters), and 11 (six parameters) remained for further analysis. Then, fits for Model 7 and 9 were selected for their lower χ^2 value than in fits for Models 8 and 10, respectively, while the fits for Models 4 and 11 are the only possible choices in classes of models with three and six parameters. The F-test (Bevington, 1969; Cook and Weisberg, 1990) for selected fits shows that Models 7, 9, and 11 are *not* statistically more adequate than Model 4 (P[4,11] = 0.40; P[4,9] = 0.29; P[4,7] = 0.38, where the numbers in parentheses stand for the respective models and P denotes the probability defined above). Therefore, the final selection was guided by the parsimony principle and yielded Model 4 (three parameters) as the most adequate description of the data.

Model 4 implies that A549 cells internalized IFN by the process characterized by a single rate constant k_{e2}. The internalized radioactivity was reduced at the rate characterized by the rate constant k_h. This process became effective after the mean delay time T_h. It is noteworthy that the presence of the delay time T_h in Model 4 significantly improved the fit in comparison to Model 1. The best-fit values for Model 1, however, are statistically equivalent to those reported by Dunne et al. (1990) for the same data analyzed by a different model which did not include T_h. Thus, it appears that radioactivity associated with IFN is eliminated from A549 cells only after a significant delay following the introduction of the ligand to cells.

Interactions of A549 cells with TNF: Single endocytotic rate with elimination of

TABLE I. Best-Fit Parameter Values for Interactions of Human Interferon-α_2a With A549 Cells*

Model	k_{e1} s^{-1}	k_{e2} s^{-1}	T_e s	k_h s^{-1}	T_h s	c cpm^{-1}	χ^2
1	0	7.4×10^{-4}	0	3.7×10^{-4}	0	0	23
		7		7			
2	0	1.0×10^{-5}	0	0	0	1.7×10^{-3}	3881
		329				22	
3	4.2×10^{-4}	0.0[a]	1890	0	0	0	2399
	30	±0.0	7				
4	0	4.5×10^{-4}	0	2.6×10^{-4}	3600	0	3.1
		24		16	29		
5	0	5.4×10^{-5}	75	0	0	2.1×10^{-4}	1963
		127	150			147	
6	6.3×10^{-4}	3.0×10^{-12}	1710	0	0	2.5×10^{-4}	329
	44	2.6×10^{7}	30			22	
7	0	4.4×10^{-4}	0	2.6×10^{-4}	3520	1.2×10^{-5}	2.7
		22		18	39	189	
8	0	8.0×10^{-4}	770	3.9×10^{-4}	1120	0	6.3
		14	25	12	64		
9	2.6×10^{-4}	4.8×10^{-4}	7400	2.7×10^{-4}	3500	0	1.9
	138	36	136	25	34		
10	0	4.4×10^{-4}	110	2.6×10^{-4}	3520	1.2×10^{-5}	2.7
		10	168	6	6	191	
11	2.7×10^{-4}	4.7×10^{-4}	7560	2.7×10^{-4}	3440	8.9×10^{-6}	1.6
	1.4×10^{8}	37	130	26	28	261	

*The best-fit values (upper rows) for each model were obtained by minimization of χ^2 (Eq. 13) for data in Figure 3a. Quantities in lower rows stand for coefficients of variability determined according to Eq. (16).

[a]Best fit value ± standard deviation (see Eq. 16).

radioactivity and inhibition of endocytosis by internalized ligand. Data in Figure 4 were used to obtain the parameters in Table II by the same procedure as in Table I. By the same deductive protocol as above, we arrived at Models 4, 8, 10, and 11 for the F-test. From $P[4,11] = 0.05$, we conclude that Model 11 is more adequate than Model 4. Model 10 is superior to Model 11 by parsimony (less parameters!). Finally, from $P[8,10] = 0.08$ it follows that Model 10 is the preferred description of the data.

From Model 10, it appears that for the particular TNF concentration under the conditions in Figure 2, A549 cells endocytosed TNF in a process characterized by a single endocytotic rate constant k_{e2} and the mean transition time T_c. (However, this time is commensurate with the first experimental point and might thus be artifactual.) It must be noted that the introduction of $c \neq 0$ improved the fit (compare Models 8 and 10). The negative value of c in Model 10 indicates that the efficiency of endocytosis was diminished by the negative feedback with the internalized ligand-receptor complex.

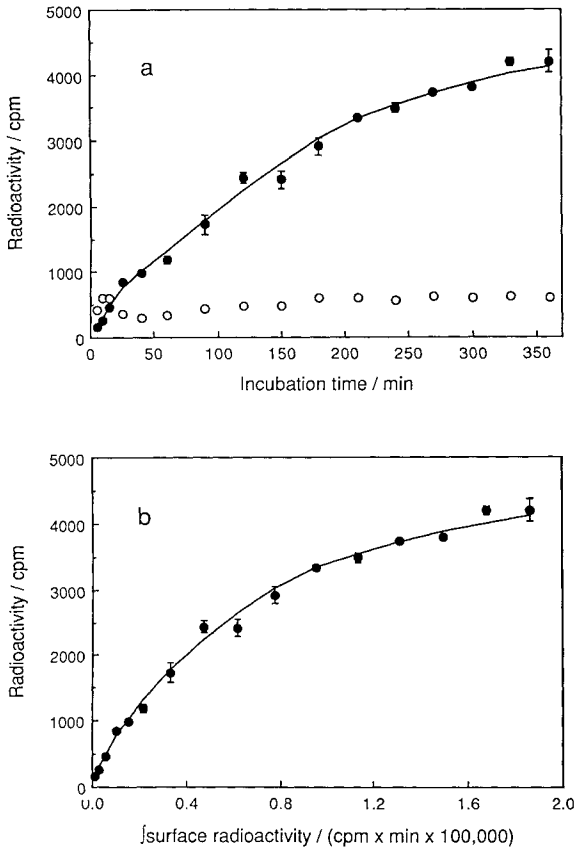

Fig. 4. Binding and internalization of ^{125}I-tumor necrosis factor-α by A549 cells. Description as in Figure 3.

The five-parameter Model 10 applied to data in Figure 4a resulted in $\chi^2 \equiv 36$ corresponding to the reduced value $\chi^2_v = 3.3$. This value compares favorably with $\chi^2_v = 6.8$ in the best fit to the same data of a classical seven-parameter model of receptor metabolism (Table I, Bajzer et al., 1989). Thus, the current model encompassing the nonlinear regulatory coupling described the data significantly better and with less parameters than the previously used models.

Interactions of A101D cells with TNF: Two endocytotic rates with elimination of radioactivity. A101D cells bind and internalize TNF (Fig. 5) as do A459 cells. However, comparison of data in Figure 4 and 5 indicates possible kinetic differences. Data in Figure 5a were analyzed by the same procedure as above. Among fits in Table III, Models 3, 5, 6, 9, 10 and 11 were selected for analysis by the F-test as they are characterized by the similarly low χ^2 values (between 52 and 64). However, the optimal model could be deduced from the a priori knowledge and by the parsimony principle. Models 3, 5, 6, and 9 were rejected for the lack of the term for elimination of radioactivity; A101D cells compare with other human epithelial tumor cells in their ability to degrade and eliminate TNF (data not shown; cf. Dunne et al., 1990). Model 9 is clearly preferred to Model 11 by the parsimony principle (fewer parameters).

The best-fit parameters for Model 9 demonstrate that the k_{c1} value was three times larger than the k_{e2} value. This finding implies a change in the rate limiting mechanism for endocytosis at T_h. To examine the role of coupling mechanisms (parameter c) in endocytosis of TNF by A101D cells, we compared the best-fit parameter values for Models 6, 9, and 10. Model 6 (c instead of k_h and T_h in Model 9) resulted in a worse fit than Model 9. Moreover, inclusion of both c and k_h (and T_h; Model 11) did not improve the fit. Thus, we conclude that the nonlinearity in Figure 5b resulted from active elimination of radioactivity rather than from attenuation of endocytosis by the internalized ligand-receptor complex.

Summary of results. Our results demonstrate that for each cell/ligand combination a different model described the data best. For interactions of A549 cells with IFN, Model 4 was the most adequate. Thus, A549 cells internalize

TABLE II. Best-Fit Parameter Values for Interactions of Human Tumor Necrosis Factor-α With A549 Cells*

Model	k_{e1} s^{-1}	k_{e2} s^{-1}	T_e s	k_h s^{-1}	T_h s	c cpm^{-1}	χ^2
1	0	1.1×10^{-3}	0	1.5×10^{-4}	0	0	237
		3		5			
2	0	1.3×10^{-3}	0	0	0	-8.8×10^{-4}	403
		4				8	
3	8.5×10^{-4}	1.7×10^{-4}	8520	0	0	0	80
	3	6	4				
4	0	8.5×10^{-4}	0	1.1×10^{-4}	7240	0	76
		3		4	8		
5	0	3.2×10^{-3}	610	0	0	-3.1×10^{-3}	182
		36	5			43	
6	8.5×10^{-4}	1.2×10^{-4}	8530	0	0	-1.5×10^{-6}	80
	7	32	10			6430	
7	0	8.2×10^{-4}	0	1.5×10^{-4}	7240	7.2×10^{-5}	73
		5		21	7	80	
8	0	9.3×10^{-4}	340	1.3×10^{-4}	6410	0	48
		12	24	13	26		
9	1.4×10^{-4}	9.3×10^{-4}	370	1.3×10^{-4}	6410	0	48
	121	11	17	12	25		
10	0	1.4×10^{-3}	520	3.6×10^{-4}	11040	-7.6×10^{-4}	36
		16	14	44	11	36	
11	0.0[a]	1.4×10^{-3}	520	3.6×10^{-5}	11040	-7.6×10^{-4}	36
	$\pm 1.7 \times 10^{-4}$	16	15	45	17	35	

*Fits for data in Figure 4a; for details see legend to Table I.
[a]Best-fit value ± standard deviation (Eq. 16)

IFN by a process characterized by a single constant. Elimination of radioactivity from cells proceeds after a significant delay (1 hour).

Model 10 was most adequate for interactions of TNF with A549 cells. As for internalization of IFN by these cells, internalization of TNF was characterized by a single rate constant. Radioactivity associated with IFN and TNF was eliminated from A549 cells with practically equal rate constants, although the onset of elimination was three times longer for TNF (3 hours). Also, incubation with TNF resulted in significant attenuation of endocytosis by the internalized ligand.

Model 9 best described the interactions of TNF with A101D cells. Here, internalization was characterized by the transition from the initially larger rate constant to the subsequently smaller rate constant. Under the conditions of experiment in Figure 5, the transition between two regimes of internalization took place 20 minutes after introduction of the ligand cells. At the same time, A101D cells started elimination of radioactivity. It is interesting that this early onset of elimination takes place devoid of the effects of the internalized ligand on the rate of endocytosis.

DISCUSSION

The power of kinetic analysis to resolve complex systems into elementary steps is based on independent evidence for these steps, in adequate statistically testable kinetic models, and in numerical methods for curve fitting. For receptor-mediated endocytosis of proteins, the basic elementary steps have been amply documented. They include receptor synthesis and turnover, ligand binding to and dissociation from the membrane receptors, translocation of receptors into coated pits, endocytosis, processing of the ligand-receptor complex and elimination of the processed ligand from cells (cf. reviews by Klausner et al., 1985; Goldstein et al., 1985). Usually these processes can be characterized by individual rate constants of the zeroth, pseudofirst, or first order which can be determined in separate experiments (cf. Wiley and Cunningham, 1981; Ciechanover et al., 1983; Lund et al., 1990; Owensby et al., 1990). In typical experiments, data are collected within minutes after introduc-

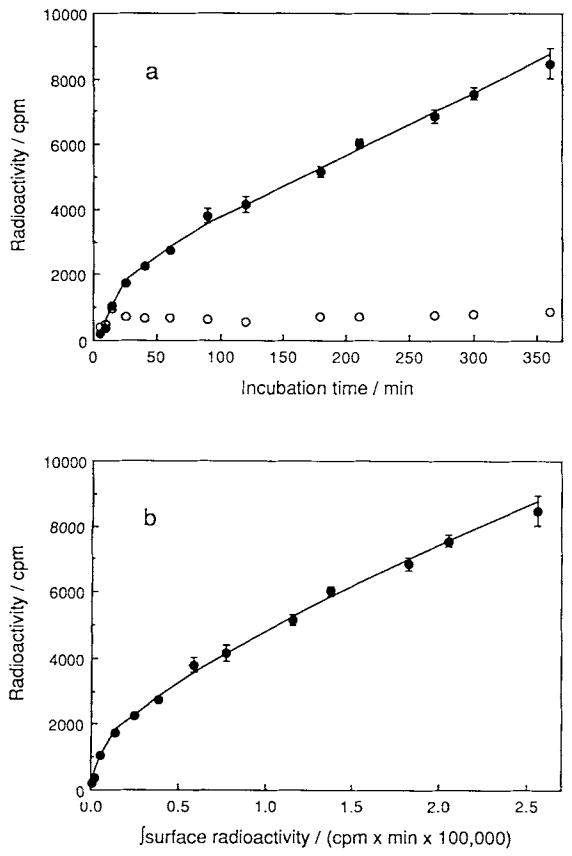

Fig. 5. Binding and internalization of ^{125}I-tumor necrosis factor-α by A101D cells. Description as in Figure 3.

tion of the ligand to cells or after rapid warming of cells pre-equilibrated with the ligand at 4°C. Usually the data are reduced by the linearization techniques.

We have been interested in ligand internalization by cells on the time scale of hours (Myers et al., 1987; Bajzer et al., 1989; Dunne et al., 1990; Lutz et al., 1990). Under such conditions, the endocytotic system exhibits complex nonlinearity in time. There have been several approaches to account for such nonlinearities by comprehensive compartmental models and to derive the relevant parameters by fitting model functions to time-dependent concentrations of surface-associated ligand and internalized ligand (Wiley and Cunningham, 1981; Ciechanover et al., 1983; Gex-Fabry and DeLisi, 1984; Lauffenburger et al., 1987; Myers et al., 1987; Beck, 1988; Bajzer et al., 1989; Waters et al., 1990). This approach has been useful (Myers et al., 1987; Nicola et al., 1988; Nicola and Metcalf, 1988; Bajzer et al., 1989; Dunne et al., 1990; Waters et al., 1990), but was limited by problems in fitting multiparameter models to data sets restricted to two experimentally determined curves only (surface-associated radioactivity and internalized radioactivity as a function of time) and by the inherent insensitivity of some parameters, particularly rate constants for binding and dissociation of the ligand (Bajzer et al., 1989; Waters et al., 1990). These problems have been compounded by the lack of user-friendly versions of the relatively complex computer software for data reduction.

To study human epithelial tumor cells interacting with IFN and TNF, we developed a simple, robust, and flexible method for analysis of processes likely to result in the observed nonlinearities. We were particularly interested in the control of the rates of endocytosis, the apparent onset of excretion of processed ligand, and the influence of internalized ligand on the rate of endocytosis. Therefore, we modeled these processes as formally independent of ligand binding and dissociation (Opresko and Wiley, 1987) to account for only two endocytotic rates separated by a transition step, for elimination of radioactivity, and for the nonlinear regulatory coupling between the internalized ligand and endocytosis. The general model included all these processes and respective parameters and was further developed into subsets of nested models for data reduction. The best-fit model was then selected for each data set on the basis of the lowest χ^2 value (verified by the F-test for nested models), the a priori knowledge of the system, and the parsimony principle.

The order of magnitude of k_e and k_h obtained in this study is consistent with the results of other studies (Wiley and Cunningham, 1981; Ciechanover et al., 1983; Gex-Fabry and DeLisi, 1984; Lauffenburger et al., 1987; Myers et al., 1987; Bajzer et al., 1989; Waters et al., 1990). However, our method can quantitate some additional features of endocytosis, such as the transition from k_{e1} to k_{e2} and the coupling between the internalized ligand and endocytosis. By the use of this method, we observed that in A549 cells the single endocytotic rate constant for TNF was larger than the single constant for IFN. This finding can be interpreted as the less restricted interactions of the TNF-receptor with the endocytotic apparatus. Endocytosis of TNF by A101D cells underwent a transition around 20 minutes that was manifest in a reduction of the endocytotic rate constant by two-thirds. This observation is compatible with the initial inter-

TABLE III. Best-Fit Parameter Values for Interactions of Human Necrosis Factor-α With A101D Cells*

Model	k_{e1} s^{-1}	k_{e2} s^{-1}	T_e s	k_h s^{-1}	T_h s	c cpm^{-1}	χ^2
1	0	1.7×10^{-3}	0	1.8×10^{-4}	0	0	308
		5		7			
2	0	3.9×10^{-3}	0	0	0	-1.5×10^{-3}	110
		10				14	
3	2.3×10^{-3}	5.0×10^{-4}	1430	0	0	0	64
	5	2	3				
4	0	1.7×10^{-3}	0	1.8×10^{-4}	1220	0	264
		4		6	1		
5	0	1.0×10^{-2}	490	0	0	-4.8×10^{-3}	61
		60	5			67	
6	2.5×10^{-3}	7.2×10^{-4}	1380	0	0	-9.3×10^{-5}	58
	5	17	4			55	
7	0	3.9×10^{-3}	0	0.0[a]	2140	-1.5×10^{-4}	110
		11		$\pm 4.2 \times 10^{-5}$	45	17	
8	0	1.7×10^{-3}	70	1.7×10^{-4}	1220	0	264
		4	50	6	1		
9	2.4×10^{-3}	8.2×10^{-4}	1290	4.5×10^{-5}	1240	0	52.2
	4	13	4	33	4		
10	0	1.0×10^{-2}	490	0.0[a]	10700	-4.7×10^{-3}	61
		42	4	$\pm$ 0.0	34	47	
11	2.3×10^{-3}	8.2×10^{-4}	1280	5.4×10^{-5}	1240	1.2×10^{-5}	52.0
	5	14	3	38	74	176	

*Fits for data in Fig 5a. For details see legend to Table I.
[a]Best fit value ± standard deviation (see Eq. 16).

nalization of a relatively large pool of receptors at the membrane. Later, the rate of endocytosis is restricted by the rate of replenishment of membrane receptors. Also, it is of interest that both cell types commenced elimination of processed ligands with a considerable delay, which was significantly shorter for IFN than for TNF in A549 cells. On the other hand, the rate constant for elimination of radioactivity associated with TNF could not be distinguished between A459 cells and A101D cells, but the process started much earlier in A101D cells. These differences indicate that the kinetics of intracellular sorting and processing of ligands and receptors depend both on the type of receptors and on the type of cells.

We built into the model the nonlinear regulatory coupling between the internalized ligand and endocytosis to account for possible inhibition ($c < 0$) or stimulation of endocytosis by internalized ligand ($c > 0$). Among possible mechanisms for these effects might be poisoning of endocytosis by the ligand and ligand-induced receptor synthesis and insertion into the membrane. It is remarkable that in interactions of A549 cells with IFN and of A101D cells with TNF there was no evidence for $c \neq 0$, indicating that the cells were not affected by internalization and processing of significant amounts of radioactive ligands. The negative value of c in Example 2 can be interpreted as characteristic of a process leading continually towards cessation of endocytosis. On the other hand, c can assume positive values only temporarily; otherwise it would result in suicide typical of positive feedbacks (cf. Riggs, 1966).

In conclusion, we observed the hitherto undetected change in the rate of endocytosis of TNF and the inhibition of endocytosis by the endocytosed ligand-receptor complex. These observations were possible by the application of the novel model of interactions of cells with protein ligands. For simplicity of the model and for flexibility of the algorithm for data reduction, we believe that the method can be applied to analysis of various formally similar processes in cellular and molecular biology, pharmacology, and toxicology. It is particularly applicable to studies of fine changes in few parameters rather than to comprehensive description of complex nonlinear systems. A user-friendly version of

the software named EndoCyte for Macintosh™ II computers is available on request.

ACKNOWLEDGMENTS

We thank Messrs. T.W. Burke and A. Zelić for technical assistance, Dr. T. Therneau and Mr. M. Marušić for help with statistical analysis, Drs. W. Lutz and R. Kumar for stimulating discussions, and Drs. J.S. Kovach and F.G. Prendergast for continuous friendly support. This work was supported in part by the NIH/NCI grant CA45312.

REFERENCES

Bajzer Ž, Myers AC, Vuk-Pavlović S (1989): Binding, internalization, and intracellular processing of proteins interacting with recycling receptors. A kinetic analysis. J Biol Chem 264:13623–13631.

Beck JS (1988): On internalization of hormone-receptor complex and receptor recycling. J Theor Biol 132:263–276.

Bender CM, Orszag SA (1978): "Advanced Mathematical Methods for Scientists and Engineers." New York: McGraw-Hill, pp 383–410.

Bevington PR (1969): "Data Reduction and Error Analysis for the Physical Sciences." New York: McGraw-Hill.

Ciechanover A, Schwartz AL, Lodish HF (1983): Sorting and recycling of cell surface receptors and endocytosed ligands: The asialoglycoprotein and transferrin receptors. J Cell Biochem 23:107–130.

Cook RD, Weisberg S (1990): Linear and nonlinear regression. In Berry DA (ed): "Statistical Methodology in the Pharmaceutical Sciences." New York: Marcel Dekker, pp 163–169.

Davis RJ, Czech MP (1986): Regulation of transferrin receptor expression at the cell surface by insulin-like growth factors, epidermal growth factor, and platelet derived growth factor. EMBO J 5:653–658.

Davis RJ, Faucher M, Racaniello LK, Carruthers A, Czech MP (1987): Insulin-like growth factor I and epidermal growth factor regulate the expression of transferrin receptors at the cell surface by distinct mechanisms. J Biol Chem 262:13126–13134.

Dunne SL, Bajzer Ž, Vuk-Pavlović S (1990): Kinetics of receptor-mediated uptake and processing of interferon-α_2a and tumor necrosis factor-α by human tumor cells. Growth Factors 2:176–177.

FitzGerald D, Pastan I (1989): Targeted toxin therapy for the treatment of cancer. J Natl Cancer Inst 81:1455–1463.

Gex-Fabry M, DeLisi C (1984): Receptor-mediated endocytosis: A model and its implications for experimental analysis. Am J Physiol 247:R768–R779.

Goldstein JL, Brown MS, Anderson RGW, Russell DW, Schneider WJ (1985): Receptor-mediated endocytosis: Concepts emerging from the LDL receptor system. Annu Rev Cell Biol 1:1–39.

Gordon P, Arakaki R, Collier E, Carpentier JL (1989): Biosythesis and regulation of the insulin receptor. Yale J Biol Med 62:521–531.

Haigler HT, Maxfield FR, Willingham MC, Pastan, I (1980): Dansylcadaverine inhibits internalization of ^{125}I-epidermal growth factor in BALB 3T3 cells. J Biol Chem 255: 1239–1241.

Jacquez JA (1985): "Compartmental Analysis in Biology and Medicine," 2nd Ed, Ann Arbor, Michigan: University of Michigan Press.

Klausner R, Van Renswoude J, Harford J, Wofsy C, Goldstein B (1985): Mathematical modeling of receptor-mediated endocytosis. In Pastan I, Willingham MC (eds): "Endocytosis." New York: Plenum. pp 259–279.

Lauffenburger D, Linderman J, Berkowitz L (1987): Analysis of mammalian cell growth factor receptor dynamics. Ann NY Acad Sci 506:147–162.

Lawson CL, Hanson RJ (1974): "Solving Least Squares Problems." Englewood Cliffs, NJ: Prentice Hall.

Lund KA, Opresko LK, Starbuck C, Walsh BJ, Wiley HS (1990): Quantitative analysis of the endocytic system involved in hormone-induced receptor internalization. J Biol Chem 265:15713–15723.

Morris, AH Jr (1981): "NSWC/DL Library of Mathematics Subroutines." Dahlgren, VA: Naval Surface Weapons Center.

Myers AC, Kovach JS, Vuk-Pavlović S (1987): Binding, internalization, and intracellular processing of protein ligands. Derivation of rate constants by computer modeling. J Biol Chem 262:6494–6499.

Nicola NA, Metcalf D (1988): Binding, internalization, and degradation of ^{125}I-multipotential colony-stimulating factor (interleukin-3) by FDCP-1 cells. Growth Factors 1:29–39.

Nicola NA, Peterson L, Hilton DJ, Metcalf D (1988): Cellular processing of murine colony-stimulating factor (multi-CSF, GM-CSF, G-CSF) receptors by normal hemopoietic cells and cell lines. Growth Factors 1:41–49.

Opresko LK, Wiley HS (1987): Receptor-mediated endocytosis in *Xenopus* oocytes. J Biol Chem 262:4116–4123.

Owensby DA, Morton PA, Schwartz AL (1989): Quantitative evaluation of receptor-mediated endocytosis. Methods Cell Biol 32:305–328.

Press WH, Flannery BP, Teukolsky SA, Vetterling WT (1986): "Numerical Recipes. The Art of Scientific Computing." Cambridge: Cambridge University Press.

Riggs DS (1966): "Control Theory and Physiological Feedback Mechanisms." Baltimore: Wilkinson and Wilkins.

Vuk-Pavlović S, Kovach JS (1989): Recycling of tumor necrosis factored receptor in MCF-7 cells. FASEB J 3:2633–2640.

Waters CM, Oberg KC, Carpenter G, Overholser KA (1990): Rate constants for binding, dissociation, and internalization of EGF: Effect of receptor occupancy and ligand concentration. Biochemistry 29:3563–3569.

Wiley HS, Cunningham DD (1981): A steady state model for analyzing the cellular binding, internalization, and degradation of polypeptide ligands. Cell 25:433–440.